

Full Length Research Paper

Synthesis and characterization of (Thallium-Tin) doped Bismuth based superconducting materials

Rashid Mahmood^{1*} and Muhammad Javed Iqbal²

¹Division of Science and Technology, University of Education, Township Lahore-54000, Pakistan.

²Centre of Nano-Science and Technology, Preston University, H-8 Islamabad.

Accepted 08 May, 2012

Doping with combinations of $Tl_{0.3-x}Sn_x$ in a certain concentration range enhances the zero resistivity temperature $T_{c(0)}$ from 104 to 108K. Both high- T_c (2223) and Low- T_c (2212) phases were detected by the X-ray diffraction analysis. However the low- T_c phase is found to dominate over the high- T_c phase with the increase in Sn content. Critical temperatures were determined by the electrical resistivity and ac magnetic susceptibility measurements. Amongst the doped samples studied here a sample containing Sn content of $x = 0.06$ exhibits comparatively the lowest value of $\Delta T = 5K$, the lowest room temperature resistivity of $\rho_{RT} = 0.01494$ ohm-cm and the highest value of $T_{c(0)} = 108K$.

Key words: Bismuth based high- T_c superconductors, X-ray diffraction, resistivity, susceptibility.

INTRODUCTION

The superconducting bismuth system $Bi_2Sr_2Ca_nCu_{n+1}O_y$ comprises multiple phases corresponding to $n = 0, 1$ and 2 with critical temperatures of 10, 85 and 110K, respectively (Maeda et al., 1988). It is one of the two main high temperature superconducting (HTS) materials from which the flexible wire or tape carrying high density of current is being manufactured for practical applications in power generation (Yi et al., 2004; Arndt et al., 2002; Fujikami et al., 2002; Balachandran et al., 1998). Doping of aliovalent impurities or oxygen non-stoichiometry can change the charge carrier concentration considerably in Bi-based system (Thamizhavel et al., 1997; Prabhakaran and Subramanian, 1997; Prabitha et al., 2005). The chemical inhomogeneity and disorder due to the doping vis-à-vis its location (site) strongly affect the critical temperature of Bi-based superconductors system (Aisaki et al., 2004). Doping of impurity atoms into HTS produces atomic level crystal defects, lattice strains, non-superconducting inclusions or precipitates and other structural defects. These inhomogeneties can improve T_c and self-field J_c which act as effective flux pinner in the system and thus enhance the J_c in applied fields (Wang

et al., 2001; Wakata et al., 1992).

Partial replacement of Bi by doping with Pb and Sb produces materials of extremely high phase purity, with Antimony playing an important role in accelerating the formation of the phase with higher superconductive transition in the Bi-Sr-Ca-Cu-O system (Cava, 2000). The role of Antimony appeared to be the enhancement of low- T_c to high T_c phase reaction beyond that achievable by Lead incorporation alone (Iqbal and Mehmood, 2006). The presence of Antimony, as Sb_2O_3 enhances the reactivity and the kinetic of reaction (especially decarbonation) as well as the promotion of the high- T_c phase (Fruth et al., 2004). By the addition of low concentrations of Sn into Bi (2223) system results in increment of T_c because it improves the weak link of grain boundary (Kim et al., 1998). Doping with (Pb-Sn) is reported to enhance J_c in materials used for practical conductors (Li et al., 2001). The enhancement of $T_{c(0)}$ by Sb-content in $Bi_{1.7}Tl_{0.3-x}Sb_xPb_{0.4}Sr_2Ca_2Cu_3O_y$ system is also reported (Iqbal and Mehmood, 2009). T_c and T_0 were found to decrease and the normal state resistance and hole concentration were observed to increase by increasing the Mo level in $Bi_2Sr_2Ca_2Cu_{3-x}Mo_xO_{10+y}$ system (Aksan and Yakinci, 2007). The presence of rare earth elements like Y, Er and Lu in bismuth based system, decreases the $T_{c(0)}$ from 109 to 104K (Pop et al., 2000).

*Corresponding author. E-mail: rashid_meh786@yahoo.com.

Pr at Ca-site helps in the formation of low-Tc Bi (2212) phase (Celebi et al., 2004). $T_{c(\text{onset})}$ and $T_{c(0)}$ decrease by doping Ni at Ca-site (Terzioglu et al., 2005). The replacement of Ca^{2+} by rare earth Sm^{3+} provides an additional electron, which, in turn decreases the hole carrier concentration which leads to decrease of $T_{c(0)}$ from = 107 to 70 K suggesting the transformation of the Bi (2223) phase into Bi (2212) phase (Mishra et al., 2000). It was found that addition of MgO in Bi (2223) system influenced the microstructure of the samples and decreased the mean size of grains (Guilmeau et al., 2003). It has been recently suggested that the substitution of Bi^{+3} by Pb^{+2} draws electronic charges out of the CuO_2 layers and thus increases the number of oxygen hole (charge carrier) in these layers (Rahaman, 2003). In the present study, binary mixtures of Tin and Thallium are added to BiPb (2223) system that enhances the value of $T_{c(0)}$ by approximately 4K. However, it was observed that Bi (2212) phase dominated the Bi (2223) phase in almost all the samples investigated here.

EXPERIMENTAL

The samples with the nominal composition $\text{Bi}_{1.7}\text{Tl}_{0.3-x}\text{Sn}_x\text{Pb}_{0.4}\text{Sr}_2\text{Ca}_2\text{Cu}_3\text{O}_y$ (where $x = 0.00, 0.02, 0.04, 0.06, 0.08, 0.10$ and 0.20) were prepared by the conventional solid-state reaction method (Maeda et al., 1988). The stoichiometric amounts of high purity Bi_2O_3 (99.9%) PbO (99.9%) Sn_2O_3 (99.9%) and SrCO_3 (99.9%), supplied by Aldrich, and CuO (>99%), CaCO_3 (99.9%) and Tl_2O_3 (>99%) supplied by Fluka, were used as starting materials. The required quantities of the materials were weighed, mixed and ground in an Agate mortar and pestle for 1 to 2 h using an electrical grinder. The mixtures were first calcined in air using a temperature programmed muffle furnace initially at 800°C for 48 h at optimized heating rate of 14°Cmin^{-1} . The resulting powders were ground and pellets of 13 mm were prepared at 95 kN. m^{-2} pressure. These pellets were sintered in air at 850°C for 96 h, 860°C for 24 h and then at 870°C for 24 h in the muffle furnace at the heating rate of $14^\circ\text{C.min}^{-1}$. The samples were allowed to cool at natural furnace cooling. The ac magnetic susceptibility of the samples was measured with laboratory-built ac susceptometer using a lock-in amplifier (Stanford SR-830). The electrical resistivity was measured with a conventional dc four-point probe method employing Janis Research Module (VPF -100) combined with a temperature controller (Lakeshore-321). High conductivity silver paint (Agar Scientific) was used for resistivity measurements. Powder X-ray diffraction patterns of the samples were obtained with (Philips X'pert PRO 3040/60) diffractometer which uses Cu K α radiation source of 40 kV and 30 mA with a step of 0.02 over the range of 7 to 70° and with a scan speed of 8°min^{-1} . The scanning electron microscopy was performed by using Joel Jsem- 6460 scanning electron microscope.

RESULTS AND DISCUSSION

Figure (a–f) shows the room temperature X-ray diffraction patterns of bismuth based superconducting materials containing different Tl:Sn ratios, that is, $\text{Bi}_{1.7}\text{Tl}_{0.3-x}\text{Sn}_x\text{Pb}_{0.4}\text{Sr}_2\text{Ca}_2\text{Cu}_3\text{O}_y$ as a result of variation of Sn content in the range of $x = 0.00$ to 0.10 . The intensity of

reflection peak (115) at $2\theta \sim 27.6^\circ$ corresponding to the low-Tc 2212 phase initially increases gradually from 885.99 to 1569.63 and to 1795.31 cps respectively, on the addition of Sn contents of $x = 0.00, 0.04$ and 0.06 and then decreases to 1694.66, 1538.39 and to 1123.94 cps, respectively for $x = 0.08, 0.10$ and 0.20 . In our previous studies where combinations of Tl: Sb were doped [26], the reflection peak (115) at $2\theta \sim 27.6^\circ$ was observed to decrease for Sb contents of $x = 0.00$ to 0.20 . The X-ray diffraction data of Sn-doped samples also reveals that the amount of low-Tc (2212) phase regularly increases from $x = 0.00$ to 0.10 , however for $x = 0.20$ a prominent peak at $2\theta \sim 33.2211^\circ$ is clearly seen for high-Tc (2223) phase which indicates that Sn content in a certain concentration range in Tl and Sn binary mixture helps in the formation of low-Tc phase while beyond certain limits it contributes to the conversion of a low Tc (2212) phase to high-Tc (2223) phase. As shown in Table 1, the other characteristic reflection peaks at $2\theta \sim 29, 31$ and 33° also correspond to the low-Tc phase and their intensity increases at a certain lower concentration range and then decreases for $x = 0.10$ and 0.20 , respectively.

Figure 2 shows the temperature versus resistivity curves for $\text{Bi}_{1.7}\text{Tl}_{0.3-x}\text{Sn}_x\text{Pb}_{0.4}\text{Sr}_2\text{Ca}_2\text{Cu}_3\text{O}_y$ samples containing different Sn contents ($x = 0.00, 0.04, 0.06, 0.08, 0.10$ and 0.20). All the samples studied in this work exhibit a metal-like behavior in the normal state region before transition to the superconducting phase. The values of the room temperature resistivity (ρ_{RT}) vary from 0.01326 to 0.02125 ohm-cm at different temperatures in the range of (77 to 300K) and evidently the sample with Sn content of $x = 0.00$ has the lowest value of 0.01326 ohm-cm. There is almost regular increase in the value of ρ_{RT} for samples containing $x = 0.00$ to $x = 0.2$ with the exception of $x = 0.06$ (Table 2). It is evident from the resistivity versus temperature plots that almost all the synthesized samples have the residual resistivity (ρ_0) of less than 0.006 ohm-cm. The observed values of $T_{c(0)}$ are in the range of (104 to 108)K as shown in Table 2. Amongst the synthesized samples, samples containing Sn contents of $x = 0.06$ and $x = 0.20$ show highest value of $T_{c(0)} = 108\text{K}$ whereas a sample with $x = 0.00$ exhibits lowest value of 104K. The values $T_{c(\text{onset})}$ are noted in the range of (112 to 117)K as given in Table 2. The sample with $x = 0.06$ show the lowest value of the transition width, $\Delta T = 5\text{K}$ which varies from 5 to 11K.

Figure 3 shows temperature versus magnetic susceptibility curves for $\text{Bi}_{1.7}\text{Tl}_{0.3-x}\text{Sn}_x\text{Pb}_{0.4}\text{Sr}_2\text{Ca}_2\text{Cu}_3\text{O}_y$ samples containing different Sn contents. AC magnetic susceptibility of the samples is measured with a frequency of 270 Hz in a temperature range of 77 to 300K. All the samples exhibit diamagnetic character and show Messiner effect. The samples show diamagnetic transition in the range of (105 to 114)K with the variation of Sn concentration. The presence of high-Tc and low-Tc phases is clearly indicated in the susceptibility curves by the deviation from the sudden and sharp decreasing

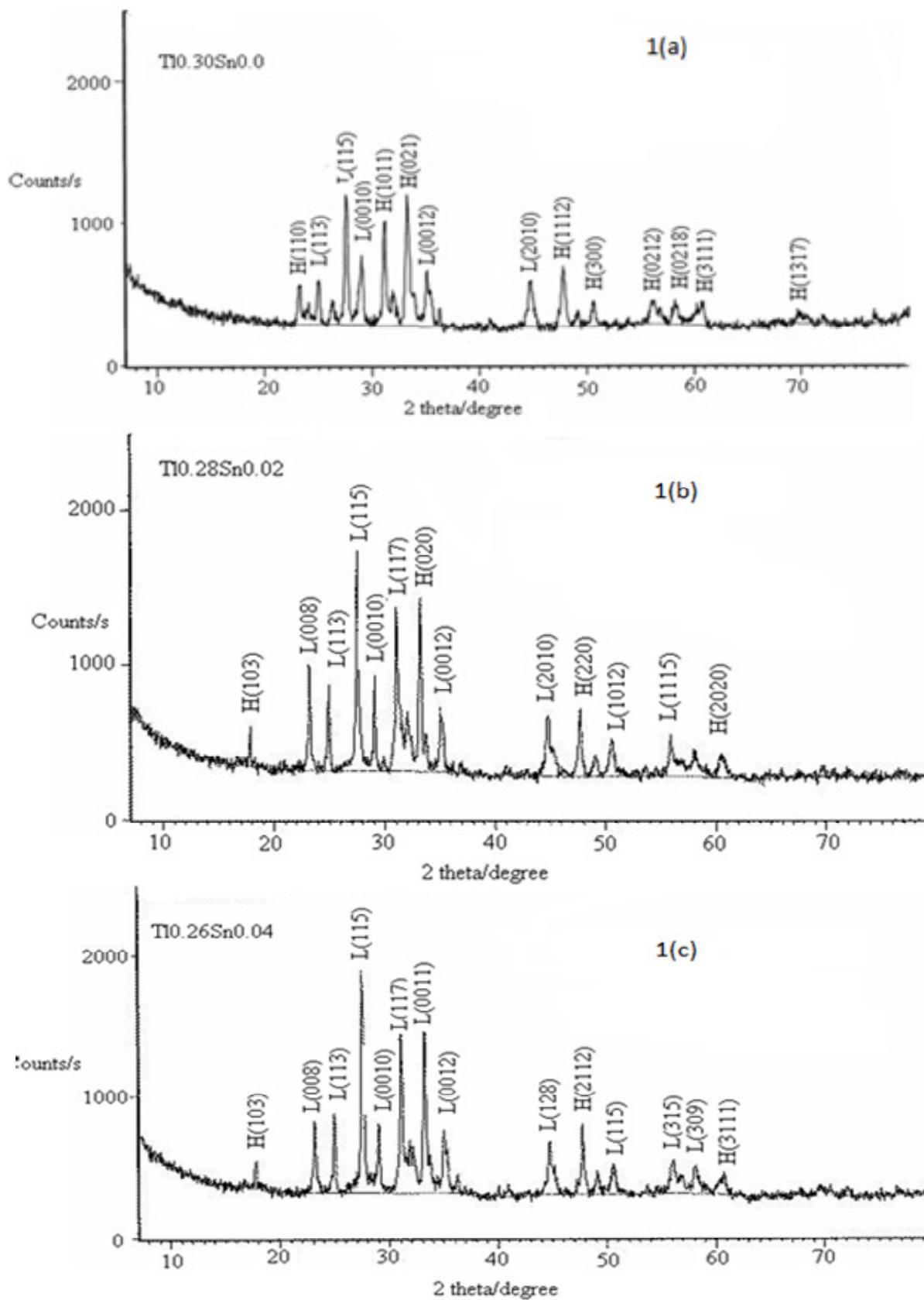


Figure 1. X-ray diffraction patterns of $Bi_{1.7}Ti_{0.3-x}Sn_xSr_2Ca_2Cu_3O_y$ samples containing Sn contents, $x =$ (a) 0.00, (b) 0.02, (c) 0.04, (d) 0.06, (e) 0.08 and (f) 0.10.

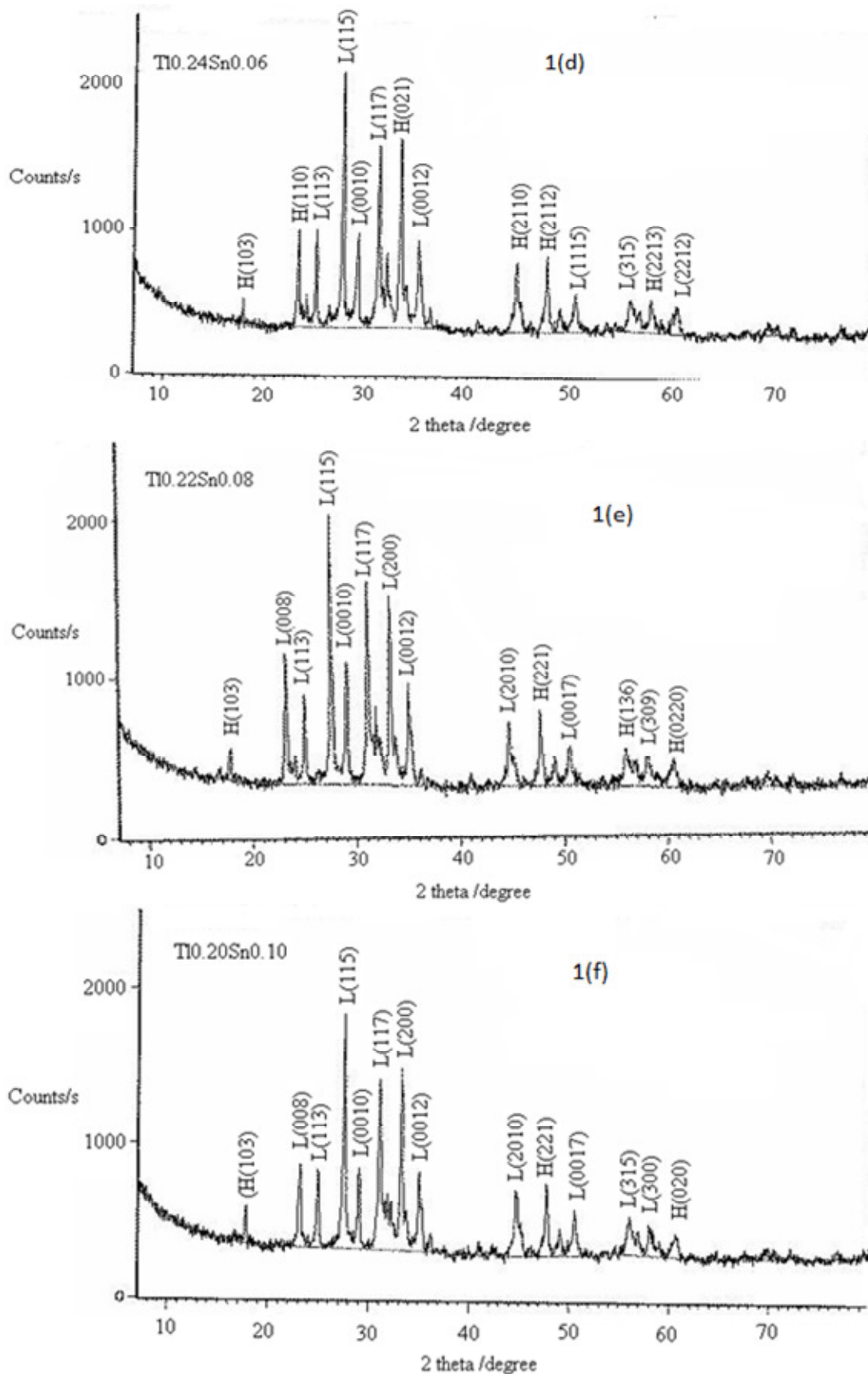


Figure 1. Contd.

Table 1. Comparison of 2θ , d- value, characteristic peak intensities, H (hkl) and L (hkl) of Tl-Sn doped samples $\text{Bi}_{1.7}(\text{Tl}_{0.3-x}\text{Sn}_x)\text{Pb}_{0.4}\text{Sr}_2\text{Ca}_2\text{Cu}_3\text{O}_y$ where $x = 0.0, 0.04, 0.06, 0.08, 0.10$ and 0.20 .

Samples	2θ	d-values	Characteristic peak intensities	Phase (hkl)	Relative intensities of highest peak intensities of low and high-Tc phases	
$\text{Bi}_{1.7}\text{Tl}_{0.3}\text{Sn}_{0.0}\text{Pb}_{0.4}\text{Sr}_2\text{Ca}_2\text{Cu}_3\text{O}_y$	27.6669	3.22433	885.99	L(1 1 5)	0.955	
	29.0865	3.07011	405.31	L(0 010)		
	31.2040	2.86644	748.33	H(011)		
	3.2931	2.69119	928.04	H(0 21)		
$\text{Bi}_{1.7}\text{Tl}_{0.26}\text{Sn}_{0.04}\text{Pb}_{0.4}\text{Sr}_2\text{Ca}_2\text{Cu}_3\text{O}_y$	27.5969	3.23234	1596.63	L(1 1 5)		
	29.0739	3.07085	483.60	L(0010)		
	31.1252	2.87351	1156.29	L(1 1 7)		
	33.2959	2.69097	1143.12	L(0011)		
$\text{Bi}_{1.7}\text{Tl}_{0.24}\text{Sn}_{0.06}\text{Pb}_{0.4}\text{Sr}_2\text{Ca}_2\text{Cu}_3\text{O}_y$	27.6480	3.22648	1795.31	L(1 1 5)		1.38
	29.1478	3.06379	651.05	L(0010)		
	31.1760	2.86894	1273.19	L(1 1 7)		
	3.3319	2.68815	1296.78	H(0 21)		
$\text{Bi}_{1.7}\text{Tl}_{0.22}\text{Sn}_{0.08}\text{Pb}_{0.4}\text{Sr}_2\text{Ca}_2\text{Cu}_3\text{O}_y$	27.5856	3.23364	1694.66	L(1 1 5)		
	29.0718	3.07163	778.25	L(0 010)		
	31.1100	2.87488	1286.24	L(1 1 7)		
	3.2767	2.69248	1199.57	L(2 0 0)		
$\text{Bi}_{1.7}\text{Tl}_{0.20}\text{Sn}_{0.10}\text{Pb}_{0.4}\text{Sr}_2\text{Ca}_2\text{Cu}_3\text{O}_y$	27.5760	3.23474	1538.39	L(1 1 5)	1.05	
	29.0494	3.07394	530.48	L(0010)		
	31.1001	2.87577	1101.79	L(1 1 7)		
	33.2861	2.69209	1158.61	L(2 0 0)		
$\text{Bi}_{1.7}\text{Tl}_{0.10}\text{Sn}_{0.20}\text{Pb}_{0.4}\text{Sr}_2\text{Ca}_2\text{Cu}_3\text{O}_y$	27.5559	3.23706	1123.94	L(1 1 5)		
	28.9573	3.08351	396.72	H(0012)		
	31.0848	2.87715	747.65	L(1 1 7)		
	33.2211	2.69686	1069.47	H(0 2 0)		

Table 2. Comparison of room temperature resistivity ρ_{RT} , critical transition temperature $T_{\text{c}}^{(\text{onset})}$, zero resistivity temperature $T_{\text{c}(0)}$ and transition width ΔT values calculated for different samples of $\text{Bi}_{1.7}\text{Tl}_{0.3-x}\text{Sn}_x\text{Pb}_{0.4}\text{Sr}_2\text{Ca}_2\text{Cu}_3\text{O}_y$ (where $x = 0- 0.20$).

Nominal composition	ρ_{RT} (ohm-cm)	$T_{\text{c}(0)}$ (K)	$T_{\text{c}}^{(\text{onset})}$ (K)	ΔT (K)
$\text{Bi}_{1.7}\text{Tl}_{0.3}\text{Sn}_{0.0}\text{Sr}_2\text{Ca}_2\text{Cu}_3\text{O}_y$	0.01326	104	114	10
$\text{Bi}_{1.7}\text{Tl}_{0.26}\text{Sn}_{0.04}\text{Sr}_2\text{Ca}_2\text{Cu}_3\text{O}_y$	0.01578	105	112	07
$\text{Bi}_{1.7}\text{Tl}_{0.24}\text{Sn}_{0.06}\text{Sr}_2\text{Ca}_2\text{Cu}_3\text{O}_y$	0.01494	108	113	05
$\text{Bi}_{1.7}\text{Tl}_{0.22}\text{Sn}_{0.08}\text{Sr}_2\text{Ca}_2\text{Cu}_3\text{O}_y$	0.01825	107	116	09
$\text{Bi}_{1.7}\text{Tl}_{0.20}\text{Sn}_{0.10}\text{Sr}_2\text{Ca}_2\text{Cu}_3\text{O}_y$	0.02125	104	117	11
$\text{Bi}_{1.7}\text{Tl}_{0.10}\text{Sn}_{0.20}\text{Sr}_2\text{Ca}_2\text{Cu}_3\text{O}_y$	0.01575	108	114	06

trend. The diamagnetic transition shifts towards lower temperature with increase in Sn content, however not in a regular order which indicates the presence of low-Tc (2212) phase in excess. The difference in sharpness and saturation level of the diamagnetic signals is due to the interconnectivity of the grains.

Figure 4 shows the scanning electron micrographs of $\text{Bi}_{1.7}\text{Tl}_{0.3-x}\text{Sn}_x\text{Pb}_{0.4}\text{Sr}_2\text{Ca}_2\text{Cu}_3\text{O}_y$ samples containing different Sn contents. A predominantly uniform phase is clearly evident in the concentration range of $x = 0.00$ to 0.08 however there is some indication of some impurity phase in the cases of the samples with $x = 0.10$ to 0.20 .

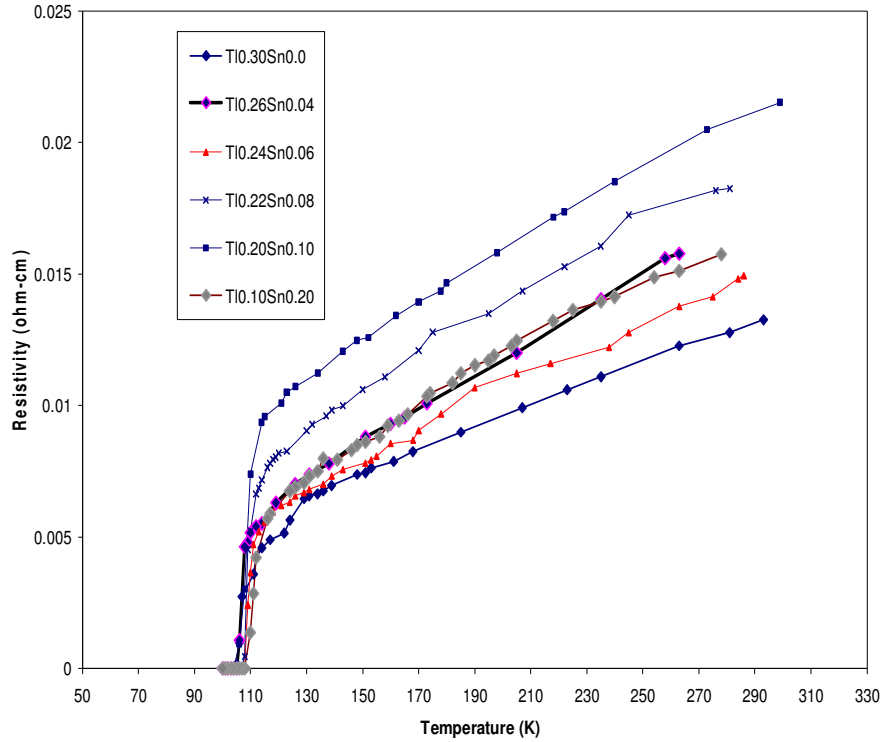


Figure 2. The dc electrical resistivity versus temperature curves of $\text{Bi}_{1.7}\text{Ti}_{0.3-x}\text{Sn}_x\text{Sr}_2\text{Ca}_2\text{Cu}_3\text{O}_y$ samples containing Sn contents, $x = 0.00, 0.04, 0.06, 0.08, 0.10$ and 0.20 .

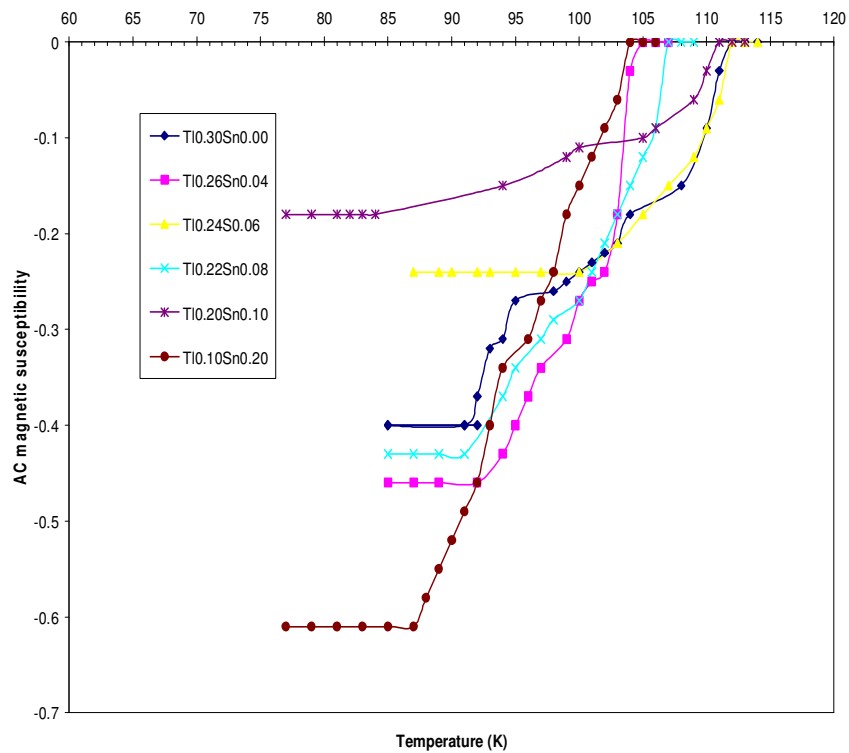


Figure 3. Ac magnetic susceptibility versus temperature curves of $\text{Bi}_{1.7}\text{Ti}_{0.3-x}\text{Sn}_x\text{Sr}_2\text{Ca}_2\text{Cu}_3\text{O}_y$ samples containing Sn contents, $x = 0.00, 0.04, 0.06, 0.08, 0.10$ and 0.20 .

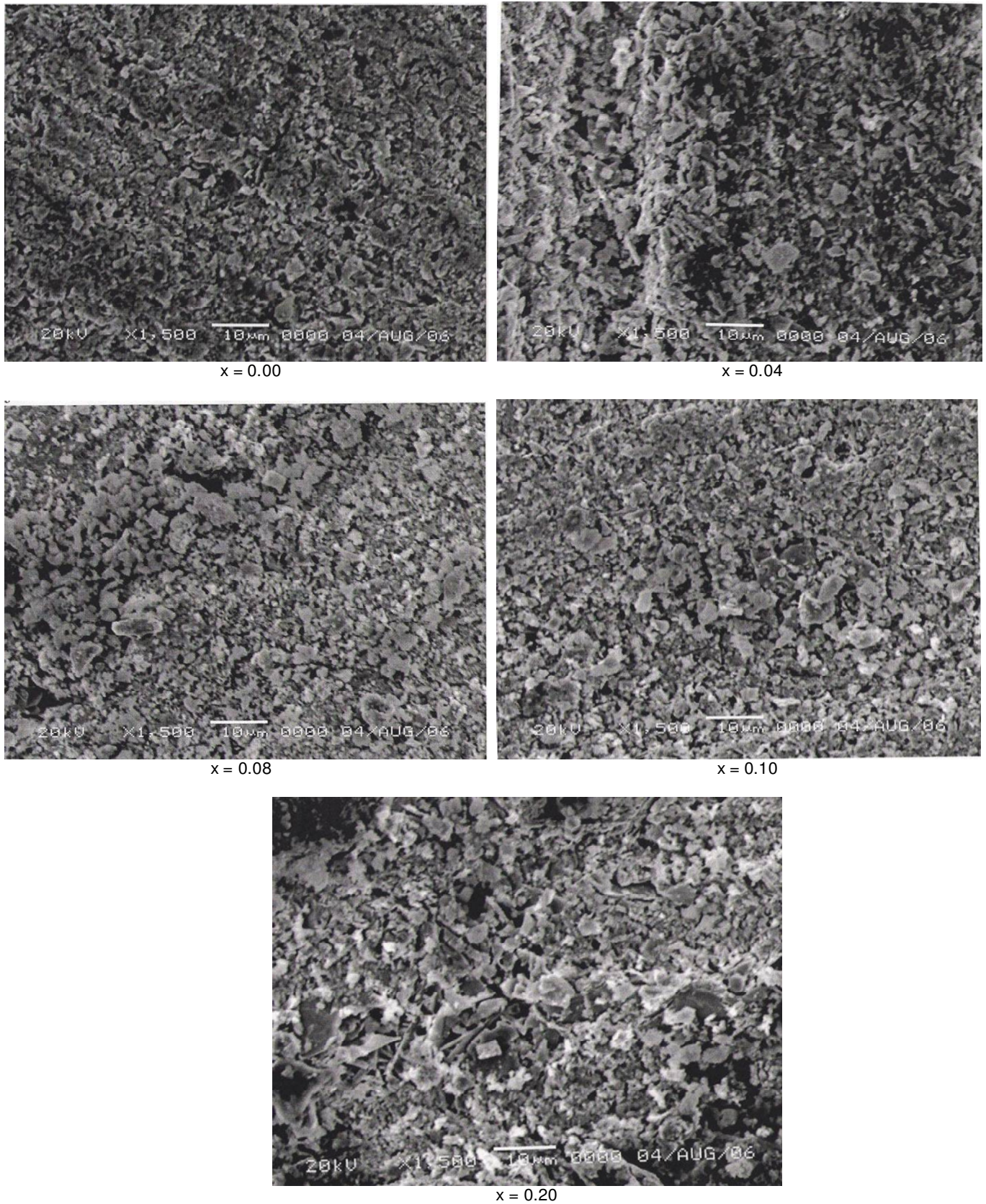


Figure 4. Scanning electron micrographs of $\text{Bi}_{1.7}\text{Ti}_{0.3-x}\text{Sn}_x\text{Sr}_2\text{Ca}_2\text{Cu}_3\text{O}_y$ samples containing Sn contents, $x = 0.00, 0.04, 0.08, 0.10$ and 0.20 .

Conclusion

Both Low- T_c (2212) and high T_c (2223) were found to be present in all the synthesized samples. Increase in Sn-concentration caused an increase in the relevant amount of Low- T_c phase. A sample with $x = 0.06$ exhibits comparatively the lowest value of $\Delta T = 5K$, the lowest room temperature resistivity of $\rho_{RT} = 0.01494$ ohm-cm and the highest value of $T_{c(0)} = 108K$.

ACKNOWLEDGEMENT

Higher Education Commission (HEC) of Pakistan is acknowledged for the financial support through indigenous 300-scholarship scheme.

REFERENCES

- Aisaki H, Kancko N, Fung DL, Damascelli A, Mang PK, Shen KM, Shen ZX, Greven M (2004). Effect of chemical inhomogeneity in bismuth-based copper oxide superconductors, *Phys. Rev. B*. 69: 064512-064519.
- Aksan MA, Yakinci ME (2007). Effect of Mo substitution on the structural and transport properties of $Bi_2Sr_2Ca_2Cu_{3-x}Mo_xO_{10+y}$ system, *J. Alloys. Comp.* 433: 22-32.
- Arndt TJ, Aubele A, Fisher B, Krauth H, Sailer B, Szulczyk A (2002). Bi-2223 tapes for applications at high temperatures and/or high fields—designs, long length processing and properties, *Physica C*, 372-376: 887- 890.
- Balachandran U, Salvamanickam V, Haldar Eror NG (1998). Development of Ag-clad Bi-2223 superconductors for electric power applications *Supercond. Sci. Technol.* 11: 978-981.
- Cava RJ (2000) Oxide Superconductors, *J. Am. Ceram. Soc.* 83: 5-28.
- Celebi S, Malik AI, Inanir F, Halim SA (2004). ac losses in Ni-doped $Bi_{1.6}Pb_{0.4}Sr_2(Ca_{1-x}Ni_x)_2Cu_3O_8$ ceramic superconductors, *Supercond. Sci. Technol.* 17: 1121-1125
- Fruth V, Popa M, Berger D, Ionica CM, Jitianu M (2004). Phases investigation in the antimony doped Bi_2O_3 system, *J. Eur. Ceram. Soc.* 24: 1295-1299.
- Fujikami J, Kaneko T, Ayai N, Kobayashi S, Hayashi K, Takei H, Sato K (2002). Development of the industrial scale Ag/Bi-2223 tape, *Physica C*, 378-381: 1061-1064.
- Guilmeau E, Andrzejewski B, Noudem JG (2003). The effect of MgO addition on the formation and the superconducting properties of Bi(2223) phase, *Physica C*, 387: 382-390
- Iqbal MJ, Mahmood R (2006), Synthesis and characterization of antimony-doped Bi-based superconducting materials”, *Mat. Sci. Eng. B*. 135: 166-171.
- Iqbal MJ, Mahmood R (2009). Improvement in high- T_c phase formation in (thallium–antimony) doped bismuth-based superconducting materials, *J. Alloys. Comp.* 477: 386-390.
- Kim HS, Jeng RA, Lee GJ, Lee DH, Ahn K, Kim KH (1998). Formation of high- T_c phase in Sn-incorporated (Bi,Pb)-Sr-Ca-Cu-O superconducting system, *Mater. Chem. Phys.* 56:147-152.
- Li Y, Kaviraj S, Berenov A, Perkins GK, Driscoll J, Caplin JAD, Cao GH, Ma QZ, Wang B, Wei L, Zaho ZX (2001). Enhancement of critical current density of (Pb,Sn)-doped Bi-2212 superconductors at high temperature, *Physica C*, 355: 51-58.
- Maeda H, Tanaka Y, Fikutommi M, Asano T (1988). A New High- T_c Oxide Superconductor without a Rare Earth Element, *Jpn. J. Appl. Phys.* 27: L209- L210.
- Mishra DR, Sharma SV, Sharma RG (2000). Role of vanadium in Bi(2223) ceramics, *PRAM. J. Phys.* 54: 317
- Pop AA, Deac IG, Ilonca G, Ciurchea Pop V (2000). *Physica B* 284-288: 1101-1102.
- Prabhakaran D, Subramanian C (1997). Metal-insulator transition in the Pr substituted Bi-2212 bulk textured crystals *Physica C*, 291: 73-78.
- Prabitha YG, Biju A, Kumar RGA, Sarun PM, Aloysius RP, Syamaprasad U (2005). Effect of Sm addition on (Bi,Pb)-2212 superconductor *Physica C*, 433: 28-36.
- Rahaman MN (2003). *Ceramic Processing and Sintering*, Marcel Dekker, Second. p.787.
- Terzioglu C, Yilmazlar M, Ozturk O, Yanmaz E (2005). Structural and physical properties of Sm-doped $Bi_{1.6}Pb_{0.4}Sr_2Ca_{2-x}Sm_xCu_3O_y$ superconductors, *Physica C*, 423: 119-126
- Thamizhavel D, Prabhakaran A, Jayavel R, Subramanian C (1997). Growth and characterization of superconducting $Bi_2Sr_2Ca_{1-x}Ce_xCu_2O_{8+\delta}$ single crystals, *Physica C*, 275: 279-283.
- Wakata M, Takano S, Munakata F, Yamauchi H (1992) Effects of cation substitution on flux pinning in Bi-2212 superconductors *Cryogenic*, 32: 1046.-1051.
- Wang XL, Liu HK, Dou SX, Horvat J, Millikon D, Heine G, Lang W, Luo HM, Ding SY (2001). Superconductivity and flux pinning in Y and heavily Pb codoped Bi-2212 single crystals, *J. Appl. Phys.* 89: 7669.
- Yi HP, Han Z, Zhang JS, Liu T, Li MY, Fang J, Liu Q, Zheng YK (2004). Research status of the manufacturing technology and application properties of Bi-2223/Ag tapes at Innost, *Physica C*, 412-414: 1073-1078.